sensors

MDPI

Article,

Highly sensitive and selective surface acoustic wave ammonia sensor operated at room temperature with a polyacrylic acid sensing layer

Weiqiang Wang[1], Yuanjun Guo[1*], Wenkai Xiong[1], Yong-Qing Fu[2], Ahmed Elmarakbi[2], Xiaotao Zu[1,*]

1 School of Physics, University of Electronic Science and Technology of China, Chengdu, 610054, P. R. China ; 202021120114@std.uestc.edu.cn(W.W.); guoyuanjun@uestc.edu.cn(Y.G.); plliu@std.uestc.edu.cn(W.X.);xztu@uestc.edu.cn(X.Z.)
2 Faculty of Engineering & Environment, University of Northumbria, Newcastle upon Tyne, NE1 8ST, UK; richard.fu@northumbria.ac.uk(Y.F.) ; ahmed.elmarakbi@northumbria.ac.uk(A.E.)
* Correspondence: guoyuanjun@uestc.edu.cn(Y.G.), xtzu@uestc.edu.cn(X.Z.)

Abstract: In this study, polyacrylic acid (PAA) films were deposited onto a quartz surface acoustic wave (SAW) resonator using a spin coating technique for ammonia sensing operated at room temperature, and the sensing mechanisms and performance were systematically studied. The oxygen-containing functional groups on the surfaces of the PAA film make it sensitive and selective to ammonia molecules, even when tested at room temperature. The ammonia molecules adsorbed by the oxygen-containing functional groups of PAA (e.g., hydroxyl and epoxy groups) increase the membrane's stiffness, which is identified as the primary mechanism leading to the positive frequency shifts. Whereas mass loading due to adsorption of ammonia molecules is not a major reason as it will result in a negative frequency shift. When the PAA coated SAW sensor is exposed to ammonia with a low concentration of 500 ppb, it shows a positive frequency shift of 225 Hz, with both good repeatability and stability, as well as a good selectivity to ammonia compared with those to C_2H_5OH, H_2, HCl, H_2S, CO, NO_2, NO, and CH_3COCH_3.

Keywords: Surface acoustic wave (SAW); Polyacrylic acid (PAA); Ammonia sensor

Citation:

Academic Editor:

Received: date
Accepted: date
Published: date

1. Introduction

Ammonia is one of the most common toxic gases and is widely used in medical, chemical, gas and food industries, and thus the risk of ammonia leakage or contamination is very high in our daily life. Excessive ammonia inhalation can lead to respiratory problems, severe headaches, sore throats, loss of smell and chest pain. Due to these potential risks, development of highly sensitive and selective ammonia sensors is of great importance [1-3]. At present, various types of ammonia sensors have been developed, including metal oxide semiconductor sensors, electrochemical sensors and surface acoustic wave (SAW) sensors [4-7], etc.

In recent years, SAW based ammonia sensors have attracted extensive attention [8-11]. They have the advantages including high sensitivity, high speed, good reliability, high precision and low cost [12-14]. A typical SAW based gas sensor is consisted of a resonator with a specific sensing film and its corresponding oscillator [15-17]. The core part is the SAW resonator [18], which is normally coated with a sensitive film, and the SAW device's resonate frequency is changed after adsorption or chemical combination of am-

monia molecules [19-20]. Changes of conductivity of the sensitive film (i.e., electrical loading), effective mass of the film (i.e., mass loading), and/or modulus of elasticity (i.e., elastic loading) can change the resonant frequency of the SAW devices [7, 16, 21].

So far, many materials have been used as sensing layers to detect ammonia gas, such as indium oxide, titanium oxide, cerium oxide, carbon nanotubes and graphene [17,22-29]. For example, Tang et al.[10] deposited ZnO/SiO_2 composite films onto the surface of SAW devices using a sol-gel method, and obtained a limit of ammonia detection of 5 ppm. Guo et al.[27] prepared SiO_2-SnO_2 sensitive thin films onto the SAW device using sol-gel and spin coating methods and obtained a limit of ammonia detection of 3 ppm. Hung et al.[29] deposited reduced graphene oxide/poly (diketopyrrolopyrrolethiophene-thieno [3,2-b]thiophene-thiophene) (rGO/DPP2T-TT) onto the SAW device using a dripping method and obtained a limit of ammonia detection of 0.5 ppm. Clearly it is crucial to find a material with a low cost and a simple method to form a sensitive film for SAW based ammonia sensors. Polyacrylic acid (PAA) polymer, a cheap organic soft matter, has a large number of carboxyl groups on its surface and forms carboxyl and ammonia ions when it is contacted with ammonia molecules. These make it a good adsorbent for toxic gases such as ammonia [30] and thus a suitable sensitive film for ammonia. Therefore, we believe that an integration of this sensing layer onto the SAW device will achieve an ammonia sensor with a high sensitivity. However, as far as we have searched, this has never been reported for SAW based ammonia sensors.

In this work, a PAA-based SAW ammonia SAW sensor was made on an ST cut quartz substrate, and its ammonia sensing mechanism operated at room temperature was studied. Results prove that the PAA SAW sensor has both good sensitivity and selectivity to ammonia when operated at room temperature.

2. Materials and Methods

2.1 SAW resonator and sensing layer

Two interdigital transducers (IDTs), each side with 30 finger pairs and reflection gratings of 100 pairs, were used to construct the SAW resonators on ST-cut quartz substrate. Using a traditional photolithography and lift-off method, the IDTs and reflection gratings were prepared with a 200 nm thick aluminum, a period of 16 μm and an aperture of 3 mm. The resonator's intrinsic frequency was designed to be 200 MHz. The configuration of the SAW resonator is schematically depicted in Figure 1.

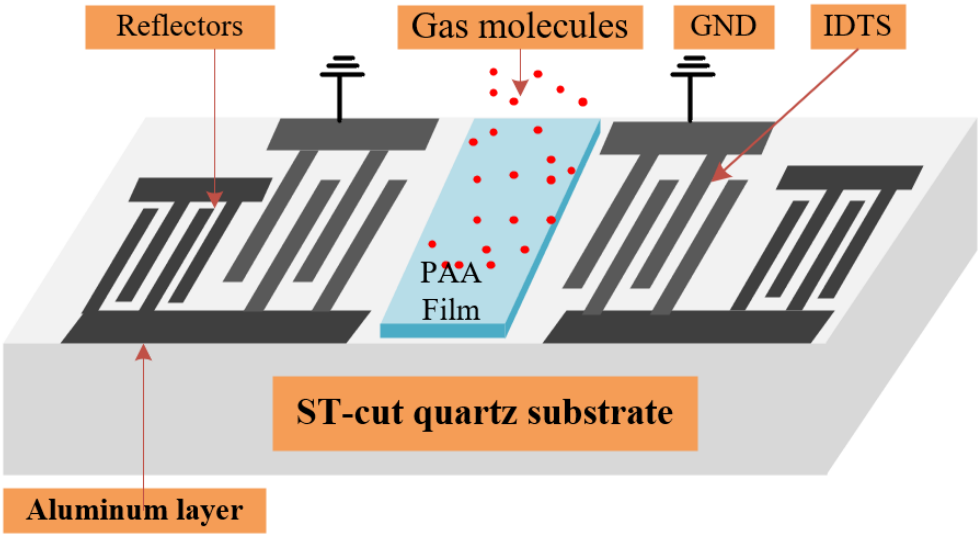

Figure 1. Schematic illustration of SAW resonator.

PAA solutions with concentrations of 0.01 M, 0.05 M, 0.1 M, and 0.2 M (bought from Chengdu Kelong Chemical Reagent Factory, China) were synthesized in a container with a magnetic stirrer at room temperature for 90 min. They were then ultrasonically agitated for two hours after being aged for 24 hours. In order to prepare a uniform PAA film, the produced PAA solutions were spin-coated onto ST-cut quartz resonators at a speed of 7000 rpm for 30 s and then dried at 60°C 0 for 8 min. Finally, the bonded aluminum wire was used to join the SAW resonator to the external circuit and control system, to form the whole SAW sensor.

2.2. Sensing and characterization platform

Figure 2 shows the gas sensing system, which mainly includes a 20 L closed chamber, a DC power supply (Agilent, E3631A), a hygro thermometer, a digital source meter (Keithley 2400) and a frequency counter (Agilent 53210A). Commercially standard gases of NH_3 (2 vol%), H_2S (2 vol%), H_2 (2 vol%), CO (2 vol%), NO_2 (2 vol%), CH_3COCH_3 (2 vol%), HCl (2 vol%) and C_2H_5OH (2 vol%) in the dry air were purchased from the China Academy of Measurement and Testing Technology. During the sensing process, the testing environment was controlled at room temperature of 20°C and 30% RH with the precise control of dried air and humidifier. The sensor was put in the 20 L closed chamber. A precisely controlled syringe was used to fill the test chamber with the given amount of ammonia. By controlling the volume of ammonia injected into the chamber, different concentrations of ammonia were obtained. For example, in an environment with 30% RH, injection of a 20 ml of standard ammonia within the 20 liters air achieved 20 ppm of ammonia.

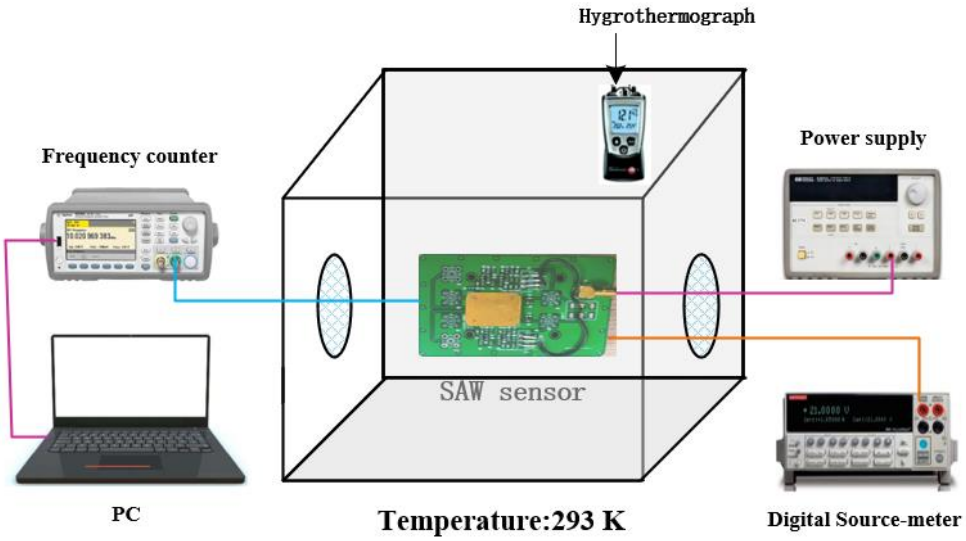

Figure 2. SAW gas sensing test system.

A field emission scanning electron microscope (FE-SEM, FEI Inspect F50), a Fourier transform infrared spectroscope (FTIR, Nicolet IS 10, Thermo Fisher Scientific) and a digital source meter (Keithley 2400) were used to characterize the morphologies, infrared absorption spectra of the prepared PAA films, and the changes in the conductance of the sensor before and after it was exposed to ammonia, respectively.

3. Results and Discussion

3.1 Characterization of sensing film

Figure 3 shows SEM images of surface and cross-section morphologies of PAA films with different concentrations. It can be seen that the prepared PAA films are quite dense, and with the concentration of PAA increased from 0.01 M to 0.2 M, the corresponding film's thickness is increased from 234.2 nm to 273.9 nm.

FTIR analysis result of PAA is shown in Figure 4. The band at 3430.16 cm^{-1} is due to O-H stretching mode and the presence of hydrogen bonding [31]. The strong band at 1711.30 cm^{-1} is due to the asymmetric stretching of –COO– [32, 33]. The bands at 1453.50 and 1414.82 cm^{-1} reveal the symmetric stretching modes of –COO– [34]. FTIR results clearly indicate that there are various hydroxyl groups and carboxyl groups on the surface of PAA film. The carboxyl groups on the PAA film were reported to have a large adsorption energy for ammonia molecules [30].

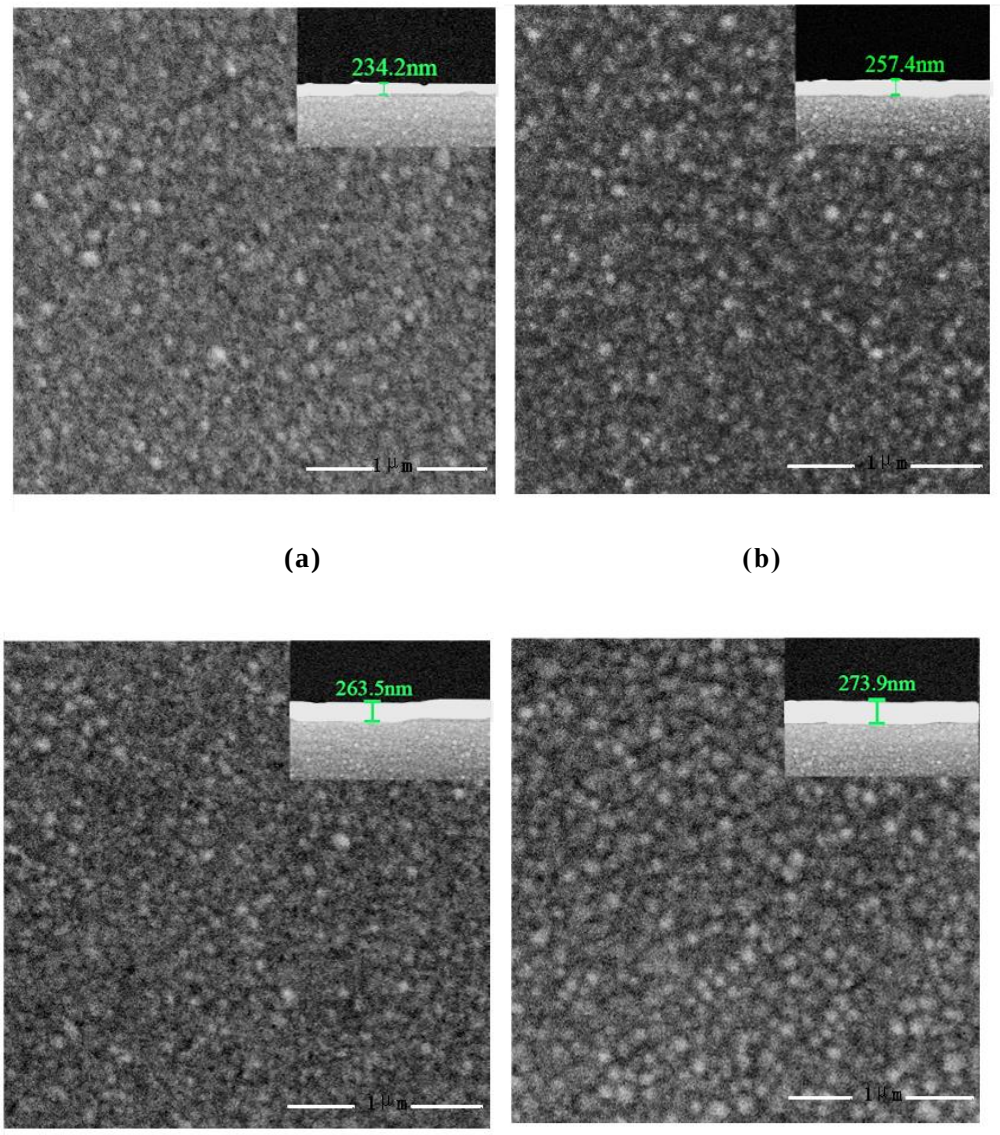

Figure 3. SEM images of surface and cross-section morphologies (inset) of PAA films with different concentrations: (a) 0.01 M; (b) 0.05 M; (c) 0.10 M; (d) 0.20 M.

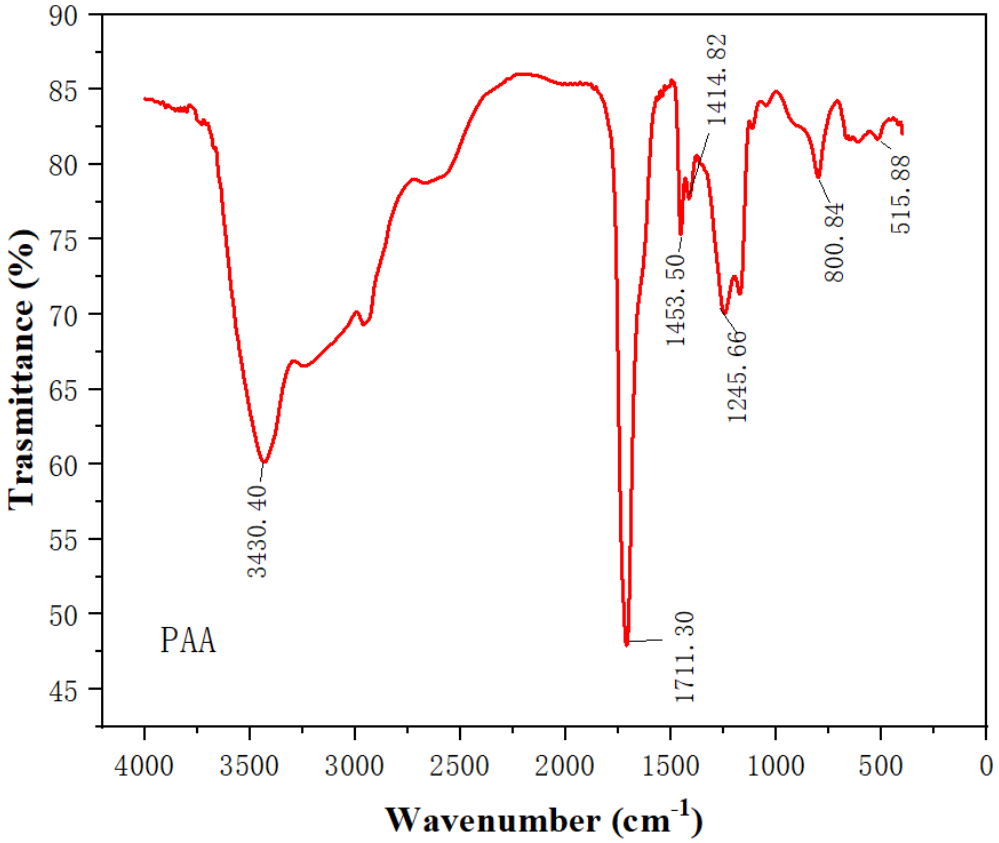

Figure 4. FTIR spectra of PAA film.

3.2 Gas sensing results and sensing mechanisms

Fig. 5 shows the frequency shifts (or the responses) of SAW sensors with sensitive films of different PAA molar ratios, when exposed to 20 ppm ammonia at 293 K and 30% RH. It can be seen from Fig. 5 that the sensor made of 0.1 M PAA solution has the largest response of 8000 Hz. Therefore, the sensor prepared with 0.1 M PAA solution was selected for the subsequent performance tests.

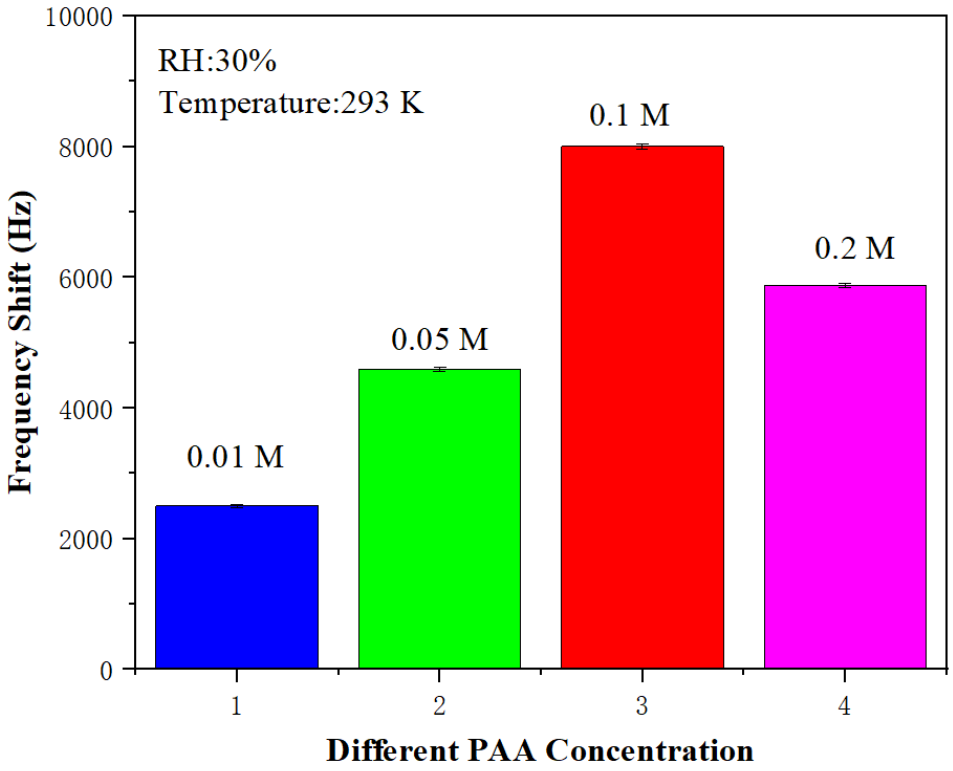

Figure5. Responses of SAW ammonia sensor prepared by PAA with different mole ratios to 20 ppm ammonia.

Fig. 6(a) shows the frequency shifts of PAA SAW sensor coated with 0.1 M PAA solution to different concentrations of ammonia between 500 ppb to 50 ppm. As can be seen from Fig. 6(a), the PAA coated SAW sensor has achieved good limits of detection (LOD) and large frequency shifts when exposed to ammonia. It has a frequency shift response of 225 Hz to 0.5 ppm ammonia. Fig. 6(b) shows the relationship between frequency shift and ammonia gas concentration. The obtained slopes of the responses for the PAA SAW sensor in the range of 0.5-2 ppm and 2-20 ppm are 750 and 400 Hz/ppm, respectively. Table 1 summarizes the LODs of SAW ammonia sensors with various sensitive layers, reported in literature, as well as that obtained from this paper. Clearly the SAW sensor with the PAA layer in this study shows one of the best LODs for the ammonia sensing compared with the others [7,10,17,21,26]. Meanwhile, the SAW sensor with the PAA layer also shows good repeatability and stability, as well as a good selectivity to ammonia, if compared with those to various gases of C_2H_5OH, H_2, HCl, H_2S, CO, NO_2, NO, and CH_3COCH_3 (seen in section 3.3).

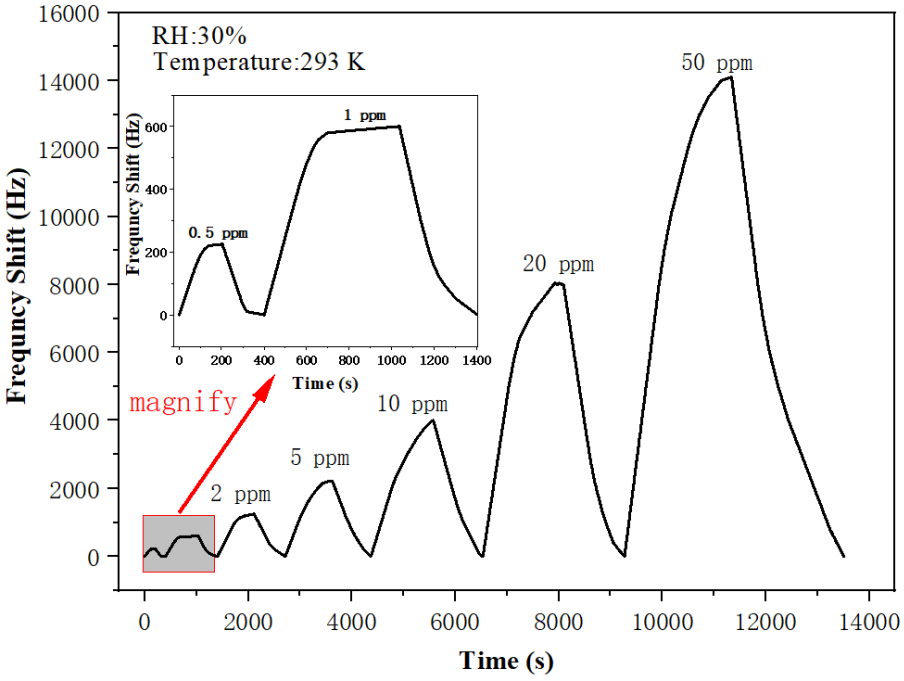

(a)

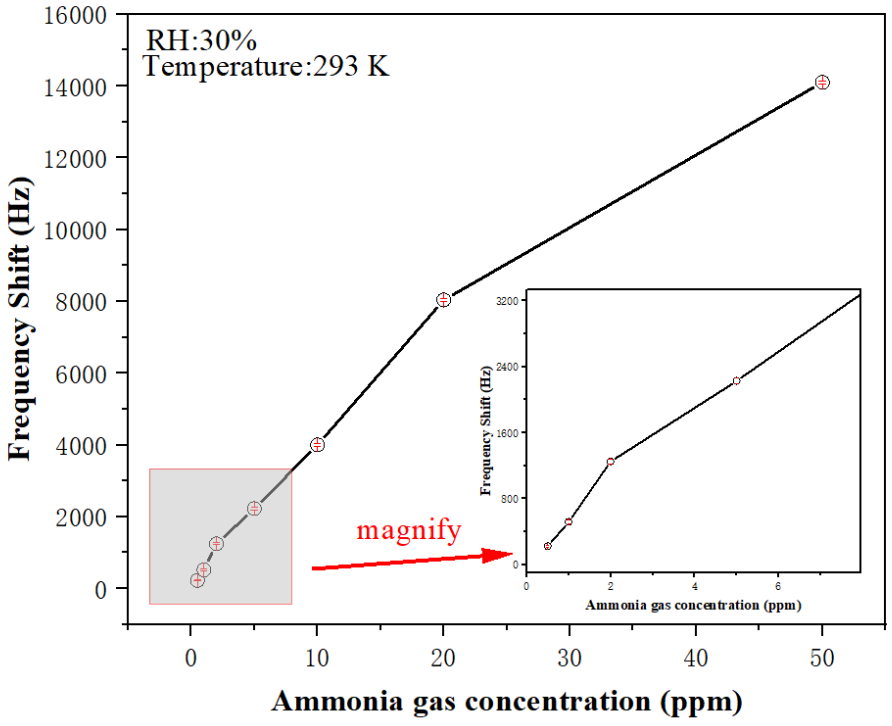

(b)

Figure 6. (a) Dynamic responses of PAASAW sensors to ammonia gases with different concentrations; (b) the relationship between frequency shift and ammonia gas concentrations.

Table 1. Summary of detection limits of various ammonia SAW sensors

Sensitive layer	Substrate	Detection limit	References
Co_3O_4/SiO_2	Quartz	1 ppm	[7]
ZnO/SiO_2 nanofilm	Quartz	5 ppm	[10]
Polyaniline film	$LiNbO_3$	25ppm	[17]
L-glutamic acid hydrochloride nanofilm	$LiNbO_3$	5 ppm	[21]
TiO_2/SiO_2 nanofilm	Quartz	1 ppm	[26]
ZnS	Quartz	1 ppm	[27]
SiO_2/SiO_2 nanofilm	Quartz	3 ppm	[28]
rGO/DPP2T-TT	Quartz	0.5 ppm	[29]
PAA film	Quartz	0.5 ppm	this work

When exposed to ammonia gases with various concentrations, the SAWS sensor's response and recovery times are quite different, which are shown in Fig. 7. Here, the response time is defined as the time needed for the sensor's frequency shift to reach 90% of its total frequency shift after being exposed to ammonia. Similar to this, the recovery time is defined as the time needed for the sensor's frequency shift to return to 10% of its total frequency shift after the release of the target gas. Results show that the response time is increased from 200 seconds to 1800 seconds, and the recovery time is increased from 230 seconds to 2400 seconds, respectively, when the ammonia concentration is increased from 0.5 ppm to 50 ppm. The gap between these two values becomes more obvious, especially at a larger ammonia concentration. This is quite easily understood because the recovery time becomes slightly longer than the response time, when the ammonia concentration is increased, thus the difference between these two values turns to be dramatically increased at a larger concentration of ammonia.

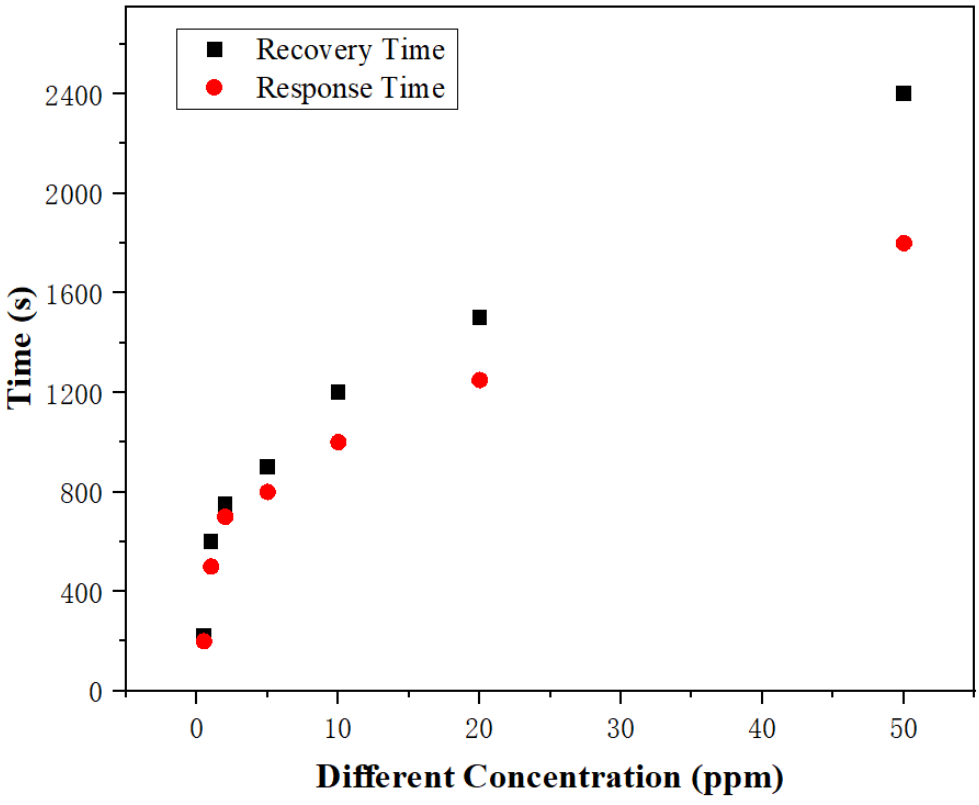

Figure 7. Response and recovery times of PAA SAW ammonia sensor at different concentrations of ammonia.

Generally speaking, there are various reasons which could result in the changes of resonant frequency of the SAW device, including electrical loading (or acoustoelectric effect), mass loading and elastic loading[26].

The relationship between frequency shift (Δf) and electroacoustic effect can be expressed using the following equation [26,35]:

$$\Delta f = -f_0 \times \frac{K^2}{2} \times \left(\frac{1}{1+\left(\frac{v_0 c_s}{\sigma_s}\right)^2} \right) \quad (1)$$

Where f_0 (~200 MHz), K^2 (0.11% for quartz), v_0 (3158 m/s for quartz) and c_s (0.5 pFcm^{-1}) are the intrinsic resonant frequency of SAW resonator, the electromechanical coupling factor, the unperturbed wave velocity for the SAW device, and the dielectric permittivity of the substrate and the environment, respectively. The measured sheet conductivity σ_s of the PAA film in air and in 20 ppm ammonia in this study are 4.6×10^{-9} S/m and 4.6138×10^{-9} S/m, respectively. The corresponding acoustoelectric parameter ($\xi = \sigma_s / v_0 C_s$) are 2.913×10^{-3}and2.921×10^{-3}, respectively, as shown in Fig. 8(a). According to Eq. (1), the original work point located at the PAA film in air, where $\Delta f_1/f_0$=-4.99995$\times 10^{-4}$; while for the work point in 20 ppm ammonia, $\Delta f_2/f_0$=-5.00014$\times 10^{-4}$. Thus, the calculated frequency shift $\Delta f = \Delta f_2 - \Delta f_1$=-(5.00014$\times 10^{-4} - 4.99995 \times 10^{-4}$) $\times f_0$=-3.8 Hz. The calculated frequency shift is only -3.8 Hz for the PAA SAW sensor exposed to 20 ppm ammonia. Compared to the experimental data in this study, it can be concluded that electroacoustic effect is not the main mechanism leading to the frequency shift of the sensor.

A SAW electrode's voltage and current were measured after the PAA film was exposed to 20 ppm of ammonia gas in order to further support this conclusion. Fig. 8(b) shows the resistance responses $R = R_{air}/R_{gas}$ of SAW device when it was exposed to 20 ppm ammonia gas, where R_{air} and R_{gas} are the resistances of the PAA film in the ambient air and in the ammonia/air mixture, respectively. As shown in Fig. 8(b), the resistance response R has no obvious changes (only from 1.000 to1.0036).

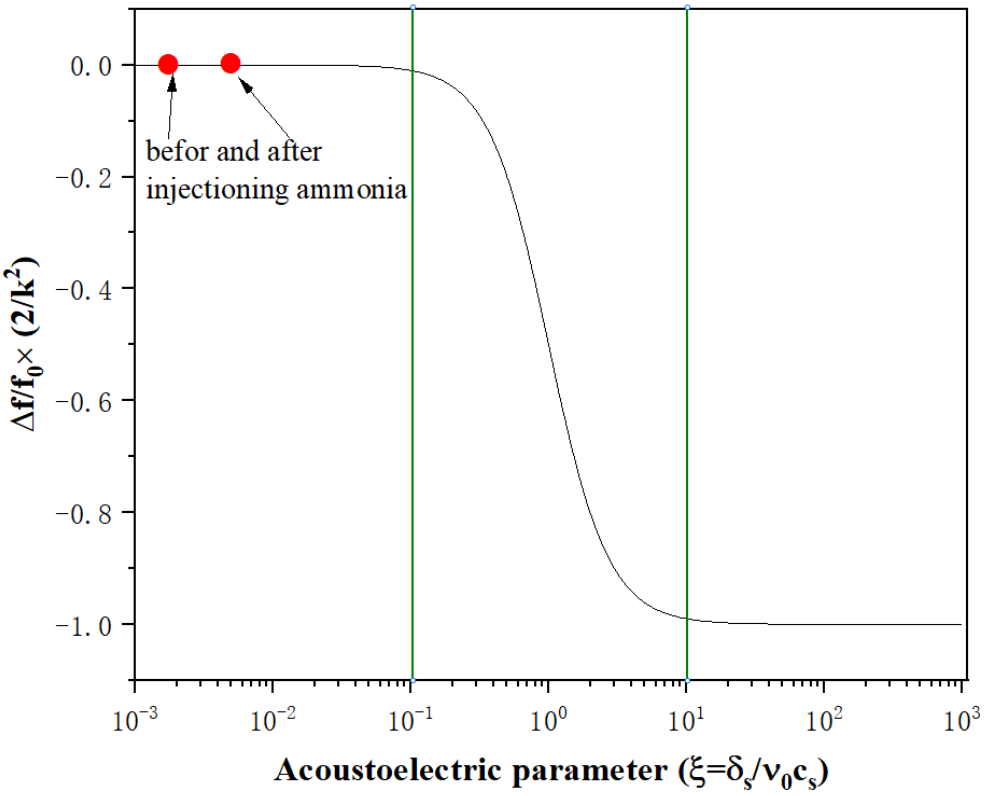

(a)

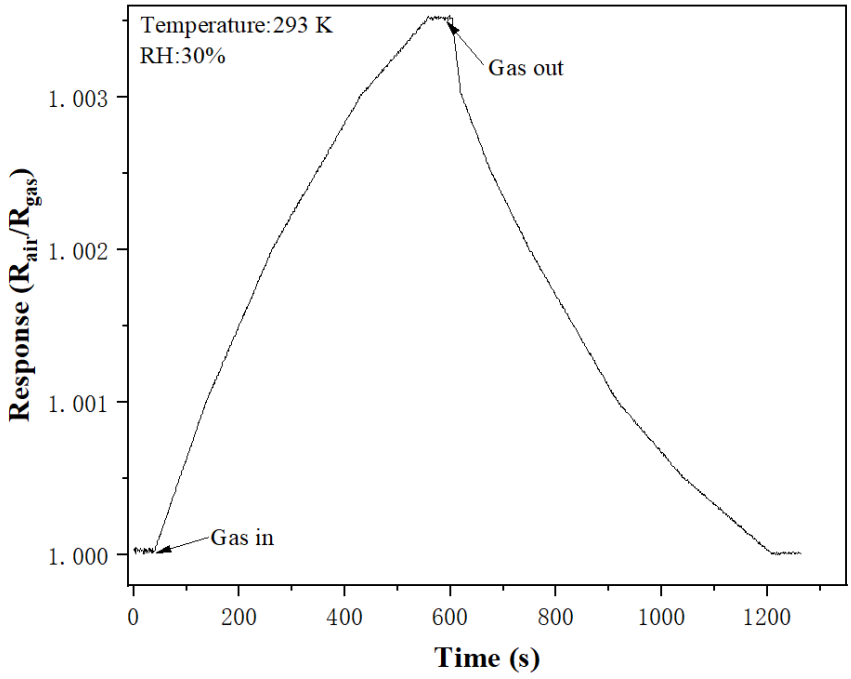

(b)

Figure8. (a) Frequency changes of PAA film SAW sensor versus acoustoelectric parameter ξ; (b) Resistance changes of PAA film before and after exposure to 20 ppm ammonia.

Effect of mass loading on the frequency shift of sensors follows Eq. (2) [26, 35]

$$\Delta f = (k_1 + k_2) \times f_0^2 \times \Delta\rho_s \quad (2)$$

where k_1(-8.7 × 10^{-8} m^{2}s kg^{-1}), k_2(-3.9 × 10^{-9} m^{2}s kg^{-1}), f_0 (~200 MHz) and $\Delta\rho_s$ are the material constants of the ST-cut quartz substrate, the intrinsic resonant frequency of SAW resonator, and the change of areal density of the sensing film under NH_3 exposure, respectively. When the PAA film is exposed to ammonia gas, a negative frequency shift can be observed because the mass density of the PAA film is increased. Therefore, the experimentally obtained positive frequency shifts in this study reveal that mass loading should not be the primary mechanism in the frequency shifts of the PAA SAW sensor to ammonia.

Effect of elastic loading on the frequency shift of sensors follows Eq. (3) [26, 35]

$$\Delta f = p\Delta E \quad (3)$$

where p and ΔE are a positive constant and the change of Young's modulus of sensing film when exposed to the NH_3 gas. The PAA has a large Young's modulus, i.e., tens of GPa [36]. Due to the small size of ammonia molecules and the three-dimensional network structure of PAA, ammonia molecules are likely to be adsorbed by the PAA. The ammonia molecules filled in the PAA gap may increase the stiffness of the membrane, thus resulting in a positive frequency shift [26]. Therefore, we can confirm that elastic loading is the main factor affecting the frequency of PAA SAW ammonia sensor.

3.3 Selectivity and stability of SAW sensors

Fig. 9 shows the selectivity of the PAA SAW sensor to several major targeted gases with a fixed concentration of 20 ppm measured at room temperature of 293 K. As can be seen from Fig. 9, the PAA SAW sensor has an obvious response to NH_3 gas and its measured value of frequency shift is as high as 8000 Hz, whereas the values for the other gases are much lower. The results show that the PAA SAW sensor has an excellent selectivity to ammonia.

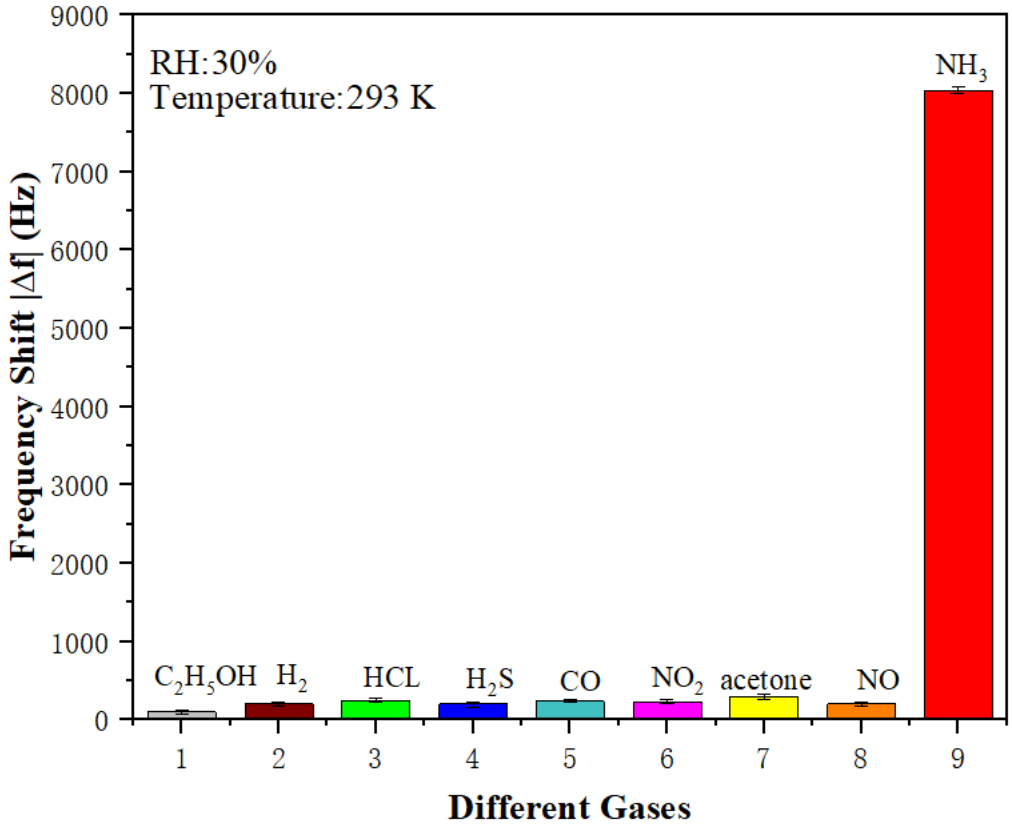

Figure 9. The absolute value of frequency shifts of PAA SAW ammonia sensor to different types of gases of 20 ppm.

Fig. 10(a) shows the dynamic responses of the sensor to five consecutive cycles of 20 ppm NH_3 exposure. The measured frequency shifts are 8.04 kHz, 8.03 kHz, 8.03 kHz, 8.04 kHz, 8.03 kHz, respectively, for these five cycles, which indicates that the PAA SAW sensor has a good short-term repeatability. In order to study long-term stability of the sensor, the sensor was tested by exposure to 0.5-20 ppm NH_3 every 4 days, up to one month. As shown in Fig. 10(b), the sensor has shown stable frequency shifts responses (less than 5%) to different concentrations of NH_3 within one month period, which shows that it has a good long-term stability.

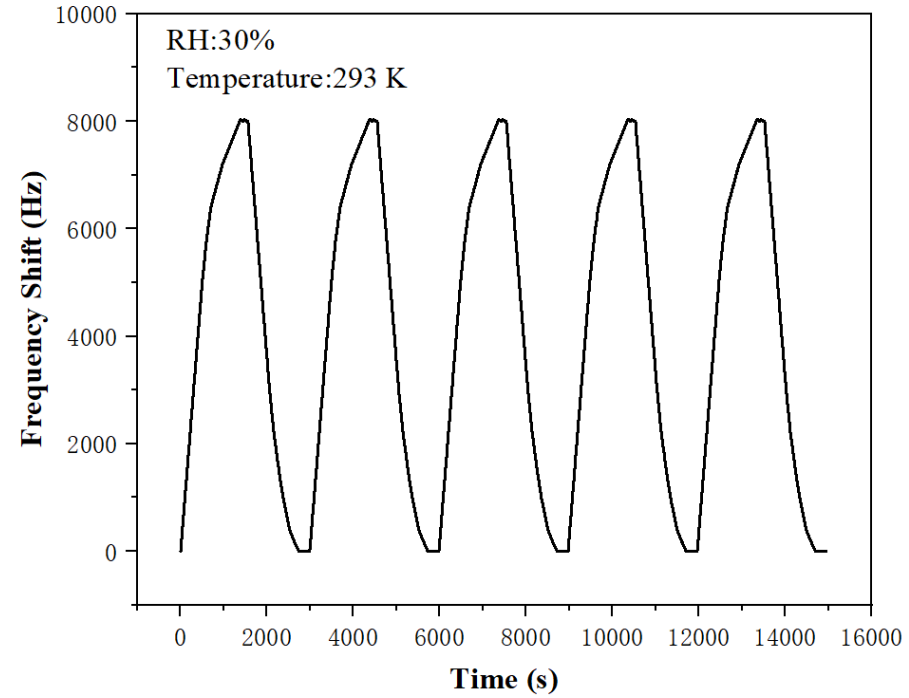

(a)

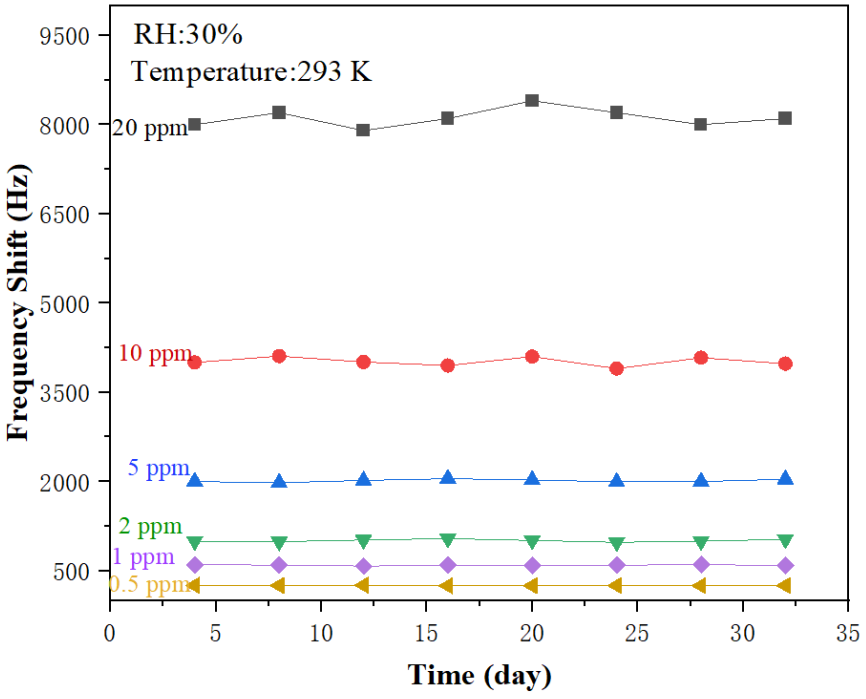

(b)

Figure 10. (a) Short-term repeatability of the PAA SAW sensor to 20 ppm ammonia;(b) Long-term stability of the PAA SAW sensor to 20 ppm ammonia.

3.4 Influences of humidity and temperature on sensing performance

Humidity is one of the important influencing parameters of SAW gas sensor. Effects of different RH levels on the properties of PAA sensitive membrane were studied and a humidifier was applied to control the relatively humidity (RH) levels in the testing chamber. Fig. 11(a) shows the sensing results of the PAA SAW sensor exposed to 20 ppm ammonia gas in different indoor environments with the RH values of 30%, 56% and 84%, respectively. In the same

concentration of ammonia, the frequency shift of the sensor decreases with the increase of RH. The reason is that with the increase of humidity, water molecules adsorbed by the hydroxyl groups in the PAA are increased, and these wate molecules can become new absorption sites because of high solubility of ammonia in water. Thus, more ammonia molecules are absorbed and the mass loading effect is increased, which leads to a larger negative frequency shift. Therefore, the total positive frequency shift is decreased. However, we should address that the effects of RH levels are not significant, which has a frequency shift of -1200 Hz when the RH level is increased from 36% to 84%.

SAW sensors are also sensitive to temperature, and their dependences can be compared using the value of temperature coefficient of frequency (TCF). The TCF value of the device can be obtained to evaluate the thermal stability of the SAW device, according to the following definitions:

$$TCF = \frac{1}{\Delta T}\frac{\Delta f}{f_0} \quad (4)$$

where ΔT, Δf and f_0 are the temperature change, the frequency change and the center frequency of the SAW device, respectively. It is well known that the TCF of ST-Cut quartz crystal is near zero [37]. Fig. 11(b) shows the variations of resonant frequencies of the PAA SAW sensor as a function of ambient temperature. When the temperature is increased from 20℃ to 70℃, the frequency shift is increased up to 500 Hz. Since the center frequency of SAW sensor is about 200 MHz, the calculated TCF is -0.049 ppm/℃, Results clearly show that the slight change of temperature has little influences on the sensor's performance and the PAA SAW ammonia sensor has an excellent thermal stability.

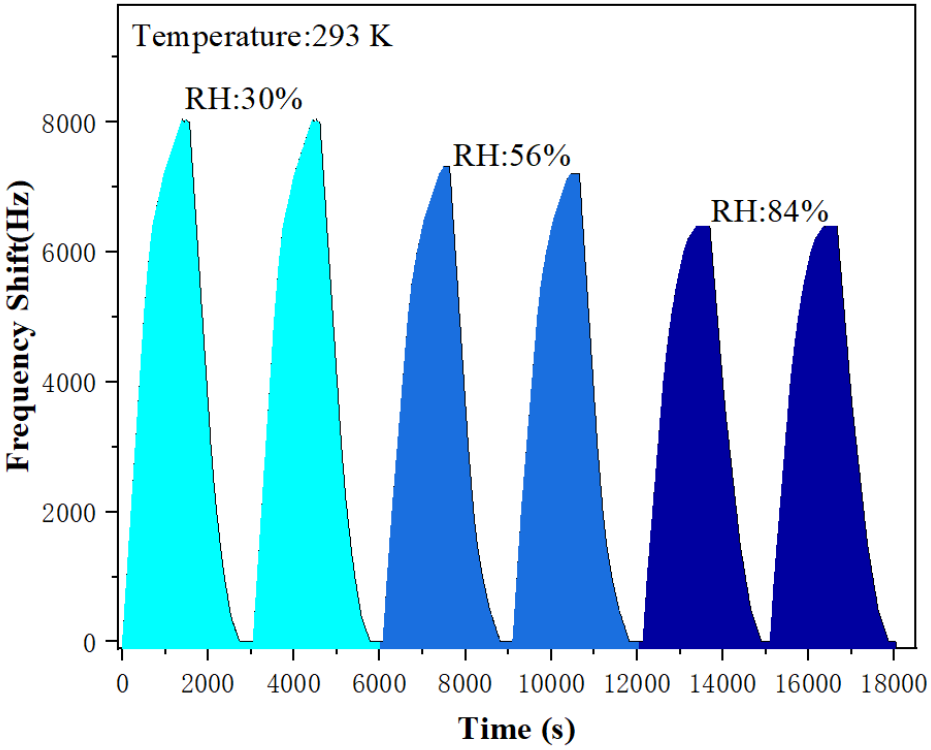

(a)

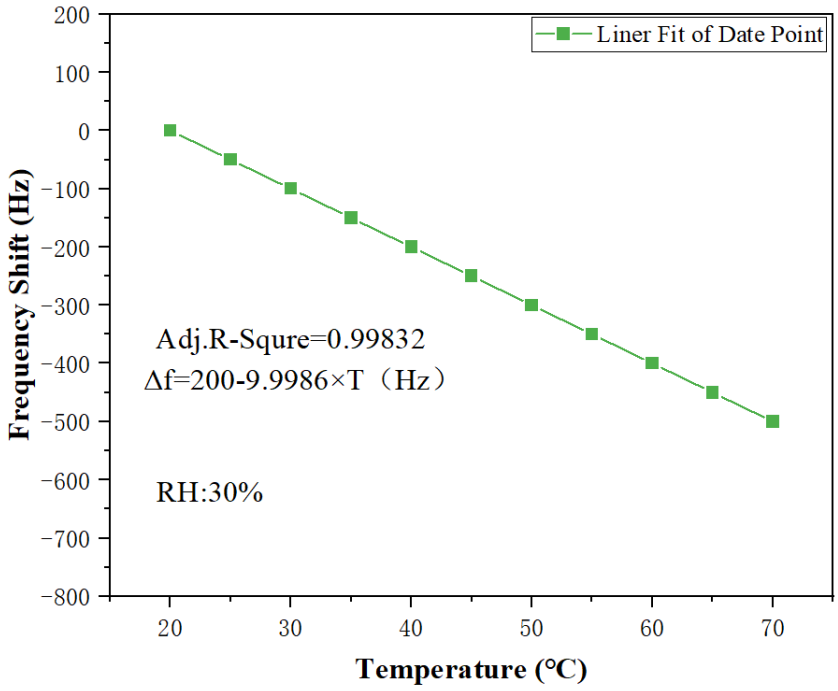

(b)

Figure 11. (a) Response-recovery curve of PAA SAW sensors to 20 ppm ammonia gas at room temperature of 293 K and different RH values; (b) The relationship between resonant frequency shift of PAA SAW sensor and temperature.

4. Conclusions

A highly sensitive and selective quartz based SAW sensor with a sensing layer of PAA film was developed to detect ammonia at room temperature, which has shown a good response to NH_3 gas molecules. The sensor has a positive frequency shift of 225 Hz when exposed to 500 ppb NH_3 gas. It has good selectivity for NH_3 and good repeatability/stability. The oxygen-containing functional groups on the surfaces of PAA film make it sensitive and selective to ammonia gas molecules, even when tested at room temperature. The ammonia molecules adsorbed by the oxygen-containing functional groups of PAA (e.g., carboxyl groups, hydroxyl) increase the membrane's stiffness, thus causing significantly elastic loading effect, which is identified as the primary mechanism leading to positive frequency shifts. The future work will be focused on significant reduction of recovery and response times, and synthesis of nanostructured PAA composite membrane in order to enhance the performance and reduce the influence of humidity on the sensing performance.

References

1. G.F. Fine, L.M. Cavanagh, A. Afonja, R. Binions, Metal oxide semi-conductor gas sensors in environmental monitoring, Sensors. 2010,10,5469-5502.
2. N. Joshi, V. Saxena, A. Singh, S. Koiry, A. Debnath, M.M. Chehimi, et al., Flexible H2S sensor based on gold modified poly-carbazole films, Sensors and Actuators B: Chemical. 2014,200,217-234.
3. J. Zhang, Z. Qin, D. Zeng, C. Xie, Metal-oxide-semiconductor based gas sensors: screening, preparation, and integration, Phys. Chem. Chem. Phys. 2017,19,6313-6329.
4. S.Y. Wang, J.Y. Ma, Z.J. Li, H.Q. Su, N.R. Alkurd, W.L. Zhou, L. Wang, B. Du, Y.Tang, D. Ao, S. Zhang, Q. Yu, X. Zu, Surface acoustic wave ammonia sensor based on ZnO/SiO_2 composite film, J. Hazard. Mater. **2015**,285,368-374.

5. B. Timmer, W. Olthuis, A. Van Den Berg, Ammonia sensors and their applications-a review, Sensor. Actuat. B-Chem. 2005,107,666-677.
6. D. Sil, J. Hines, U. Udeoyo, E. Borguet, Palladium nanoparticle-based surface acoustic wave hydrogen sensor, ACS Appl. Mater. Interfaces 2015,10,5709-5714.
7. Y.L. Tang, Z.J. Li, J.Y. Ma, H.Q. Su, Y.J. Guo, L. Wang, B. Du, J. Chen, W. Zhou, Q. Yu, X.T. Zu, Highly sensitive room-temperature surface acoustic wave (SAW) ammonia sensors based on Co3O4/SiO2 composite films, J. Hazard. Mater. 2014,280,127-133.
8. Shen CY, Huang CP, and Huang WT. Gas-detecting properties of surface acoustic wave ammonia sensors. Sensor. Actuat. B-Chem. 2004,101,1-7.
9. W. Jakubik, Elemental theory of a SAW gas sensor based on electrical conductivity changes in bi-layer nanostructures, Sensor. Actuat. B-Chem. 2014,203,511–516.
10. Y.L. Tang, Z.J. Li, J.Y. Ma, Y.J. Guo, Y.Q. Fu, X.T. Zu, Ammonia gas sensors based on ZnO/SiO_2 bi-layer nanofilms on ST-cut quartz surface acoustic wave devices, Sensor. Actuat. B-Chem. 2014,201,114–121.
11. Y.Q. Fu, J.K. Luo, X.Y. Du, A.J. Flewitt, Y. Li, G.H. Markx, A.J. Walton, W.I. Milne, Recent developments on ZnO films for acoustic wave based bio-sensing and microfluidic applications: a review, Sensor. Actuat. B-Chem. 2010,143,606–619.
12. Varghese, D. Gong, W.R. Dreschel, K.G. Ong, C.A. Grimes, Ammonia detection using nanoporous alumina resistive and surface acoustic wave sensors, Sensor. Actuat. B-Chem. 2003,94,27–35.
13. C.Y. Shen, S.Y. Liou, Surface acoustic wave gas monitor for ppm ammonia detection, Sensor. Actuat. B-Chem. 2008,131,673–679.
14. V.B. Raj, A.T. Nimal, Y. Parmar, M.U. Sharma, K. Sreenivas, V. Gupta, Crosssensitivity and selectivity studies on ZnO surface acoustic wave ammonia sensor, Sensor. Actuat. B-Chem. 2010,147,517–524.
15. W.Wang, S.T. He, S.Z. Li, M.H. Liu, Y. Pan, Enhanced sensitivity of SAW gas sensor coated molecularly imprinted polymer incorporating high frequency stability oscillator, Sensor. Actuat. B-Chem. 2007,125,422–427.
16. A.J. Ricco, S.T. Martin, T.E. Zipperian, Surface acoustic wave gas sensor based on film conductivity changes, Sensor. Actuat. 1985,8,319-333.
17. D.Y. Gallimore, P.J. Millard, M. Pereira da Cunha, Monitoring polymer properties using shear horizontal surface acoustic waves, ACS Appl. Mater. Interfaces. 2009,10,2382-2389.
18. R. Lucklum, C. Behling, P. Hauptmann, Role of mass accumulation and viscoelastic film properties for the response of acoustic-wave-based chemical sensors, Anal. Chem. 1999,71,2488–2496.
19. D. Sil, J. Hines, U. Udeoyo, E. Borguet, Palladium nanoparticle-based surface acoustic wave hydrogen sensor, ACS Appl. Mater. Interfaces. 2015,10,5709–5714.
20. Z. Y. Tang, J. Li, L. Ma, J. Wang, B. Yang, Q. Du, X. Zu Yu, Highly sensitive surface acoustic wave (SAW) humidity sensors based on sol-gel SiO_2 films: investigations on the sensing property and mechanism, Sensor. Actuat. B-Chem. 2015,215,283-291.
21. Chi-Yen Shen, Chun-Pu Huang, Hsu-Chi Chuo,The improved ammonia gas sensors constructed by l-glutamic acid hydrochloride on surface acoustic wave devices, Sensor. Actuat. B-Chem. 2002,84,231-236.
22. L. Dai, Y.G. Liu, W. Meng, G.X. Yang, H.Z. Zhou, Z.X. He, Y.H. Li, L. Wang, Ammonia sensing characteristics of $La_{10}Si_5MgO_{26}$-based sensors using In_2O_3 sensing electrode with different morphologies and CuO reference electrode, Sensor. Actuat. B-Chem. 2016,228,716-724.
23. J.Q. Wang, Z.J. Li, S Zhang, S.G. Yan, B.B. Cao , Z.G. Wang, Y.Q. Fu, Enhanced NH_3gas-sensing performance of silica modified CeO_2 nanostructure based sensors. Sensor. Actuat. B-Chem. 2018,255,862-870.
24. T. Zhang, M.B. Nix, B.-Y. Yoo, M.A. Deshusses, N.V. Myung, Electrochemically functionalized single-walled carbon nanotube gas sensor, Electroanalysis. 2006,18,1153-1158.
25. W. Meng, L. Dai, W. Meng, H. Zhou, Y. Li, Z. He, L. Wang, Mixed-potential type NH_3 sensor based on TiO_2 sensing electrode with a phase transformation effect, Sensor. Actuat. B-Chem. 2017,240,962-970.
26. Y.L. Tang, D.Y. Ao. W. Li, X.T. Zu, S. Li, Y.Q. Fu, NH_3 sensing property and mechanisms of quartz surface acoustic wave sensors deposited with SiO_2, TiO_2, and SiO_2-TiO_2 composite films, Sens. Actuators B: Chem. 2018,254,1165-1173.
27. Y. J. Guo; G.D. Long; Y.L. Tang et al., Surface acoustic wave ammonia sensor based on SiO_2-SnO_2composite film operated at room temperature. Smart Materials and Structures 2020,29, 095003.
28. G. D. Long Y. J. Guo, W. Li et al., Surface acoustic wave ammonia sensor based on ZnS mucosal-like nanostructures. Microelectronic Engineering 2020,222, 111201.
29. T. T. Hung, M. H. Chung, J. Y. Wu, C. Y. Shen, A Room-Temperature Surface Acoustic Wave Ammonia Sensor Based on rGO/DPP2T-TT Composite Films. Sensors 2022,22, 145280.
30. Ding B, Kikuchi M, Yamazaki M, and Shiratori S. Ammonia sensors based on electrospun poly (acrylic acid) fibrous membranes. IEEE Sensors 2004 Conference. Vienna Univ Technol, Vienna 2004,685-688.
31. Zhang SJ, Shi QT, Christodoulatos C, and Meng XG. Lead and cadmium adsorption by electrospun PVA/PAA nanofibers: Batch, spectroscopic, and modeling study. Chemosphere. 2019,233,405-413.

32. Manavi-Tehrani, M. Rabiee, M. Parviz, M. R. Tahriri, Z. Fahimi, in 12th European-Polymer-Federation Congress. 2009,296,457-465.
33. Wang YS, Shen YB, Zhang YW, Yue B, and Wu CX. pH-sensitive polyacrylic acid (PAA) hydrogels trapped with polysodium-p-styrenesulfonate (PSS). Journal of Macromolecular Science Part B-Physics. 2006,45,563-571.
34. Kumeta K, Nagashima I, Matsui S, and Mizoguchi K. Crosslinking reaction of poly(vinyl alcohol) with poly(acrylic acid) (PAA) by heat treatment: Effect of neutralization of PAA. Journal of Applied Polymer Science. 2003,90,2420-2427.
35. A.J. Ricco, Stephen, J. Martin, Thin metal film characterization and chemical sensors: monitoring electronic conductivity, mass loading and mechanical properties with surface acoustic wave devices, Thin Solid Films. 1991,206,94–101.
36. Yu, Q. B., Wang, X. F., Shen, Y. H., Tao, Y. L. & Xie, A. J. Preparing and physicochemical properties of microcrystalline poly-acrylic acid gels. Russian Journal of Physical Chemistry A. 2013,87,2100-2104.
37. Devkota, J.; Jagannath, P.; Ohodnicki, D. SAW Sensors for Chemical Vapors and Gases. Sensors 2017, 17, 801.